TSINGHUA SCIENCE AND TECHNOLOGY
ISSN 1007-0214 09/21 pp43-48
Volume 14, Number S2, December 2009

A Compact Piezoelectric Stack Actuator and Its Simulation in Vibration Control*

WANG Wei (王 巍)**, YANG Zhichun (杨智春)

School of Aeronautics, Northwestern Polytechnical University, Xi'an 710072, China

Abstract: To exert strong actuating power of piezoelectric stack and facilitate the incorporation of piezoelectric stack and host structure for vibration control application, a Π shape piezoelectric stack actuator (PISA) was designed. One piezoelectric stack and a Π shape metal pedestal were assembled together by a screw to build a PISA. Formula for calculating the actuating moment output of PISA was derived. Then PISA was applied in a vibration control system of a cantilever beam example. Thermal-elasticity analogy theory was applied in the modeling of the piezoelectric active vibration control system. Positive position feedback (PPF) control, linear quadric regulator (LQR) control, and neural network predictive (NNP) control strategies were adopted to perform the first bending mode vibration control of the beam. Simulation results indicate that with this new actuator and the PPF or LQR control strategy, the first bending mode amplitude of the cantilever beam can be reduced by about 60% or 79%, while using the NNP control strategy the amplitude can be suppressed by more than 95%. These results indicate that PISA can sever as a high efficiency actuator in structural vibration control application.

Key words: piezoelectric active vibration control; thermal-elasticity analogy theory; Π shape piezoelectric actuator (PISA)

Introduction

Piezoelectric stack was first proposed in 1962 by Ramsay and Mugridge[1] right after the appearance of piezoceramic materials which made relatively high-strain transducers feasible. But piezoelectric stack was not systematically studied until the late of 1970s. In 1977, Bindal and Chandra investigated the actuating performance of piezoelectric stack[2]. Later, this kind of piezoelectric component became more and more widely used in scientific research applications.

Generally, the actuating power of piezoelectric stack is much stronger than piezoelectric patch and other piezoelectric components. Due to this advantage, piezoelectric stack has great potential to become a high performance actuator for structural vibration control application. But compared with patch, stack is not convenient to be incorporated with host structures. In practice, various external components were designed to facilitate the incorporation of piezoelectric stack with the structure to be controlled[3-7]. These external components usually have complex configuration and lever systems, which cost a lot in manufacture.

In the present study, a Π (pi) shape piezoelectric stack actuator (PISA) was proposed to exert the strong actuating power of piezoelectric stack, solving the incorporation difficulty of piezoelectric stack with host structure for vibration control application. The relationship between actuating moments of PISA and driving voltage was derived. PISA was also adopted in

Received: 2009-05-08; revised: 2009-06-20

* Supported by the National Natural Science Foundation of China (No. 50375122) and the Project of New Century Excellent Talents of China (No. NCET-04-0965)

** To whom correspondence should be addressed.
E-mail: wangwei19@mail.nwpu.edu.cn; Tel: 86-29-88460461

vibration control of a cantilever beam. Thermal-elasticity analogy theory was used in the finite element modeling of the cantilever beam with PISA bonded on its root. State space model was established for the piezoelectric active vibration control system. Positive position feedback (PPF), linear quadric regulator (LQR), and neural network predictive (NNP) control strategies were applied to design the controllers of the vibration control systems. Simulation results show that PISA has the ability to seve as a high efficiency actuator in structural active vibration control application.

1 PISA Design

When a driving voltage is applied to a piezoelectric stack, expansion or contraction along the axial direction of the stack will be induced because of the inverse piezoelectric effect. If the stack is constrained at its two ends, actuating moments will be generated at the constrained foundation. Based on this theory, a special shape pedestal was designed as an installation platform and external lever for piezoelectric stack to compose a new type of actuator. By constraining longitudinal deformation of the stack, PISA can output bending moments acting on host structure through the pedestal working as the mechanical lever. The sketch of the design is shown in Fig. 1.

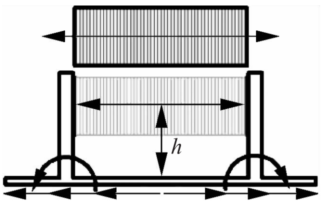

Fig. 1 PISA sketch

Because the pedestal has the shape of Greek letter Π, the new actuator is named Π shape piezoelectric actuator. As shown in Fig. 2 the new actuator consists of two main components, the piezoelectric stack and the Π shape metal pedestal. The two main components of PISA are assembled together by a screw, so the stack can be reloaded conveniently. The PISA has a flat bottom which provides an ideal installation surface for its incorporation with the host structure.

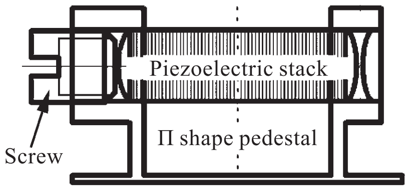

Fig. 2 Detailed design of PISA

2 Actuating Moment of PISA

Assume that a driving voltage V is applied on piezoelectric stack, and expands along its axial direction. The two ends of the stack are constrained by the Π shape pedestal with a screw. If the base of pedestal is bonded on host structure surface, actuating moments will be exerted on the structure.

Furthermore, assume p to be the pre-compression force applied on the stack. The induced deflection along the thickness direction of each piezoelectric wafer of the stack can be obtained by the following equation[8]:

$$\delta_3 = S_{33}tp / A_{\mathrm{s}} + d_{33}V \tag{1}$$

where S_{33} is the flexible coefficient of piezoelectric material under a constant driving voltage, d_{33} is the piezoelectric strain constant, t is the thickness of a single wafer. A_{s} is the area of the wafer which is also the cross section area of the stack.

Then the deformation of the entire stack can be described as

$$\delta_{\mathrm{s}} = n\delta_3 = n(S_{33}tp / A_{\mathrm{s}} + d_{33}V) \tag{2}$$

where n is the number of the piezoelectric wafers of the stack. The strain on the cross section of the stack can be obtained by

$$\varepsilon_{\mathrm{s}} = \frac{\delta_{\mathrm{s}}}{l_{\mathrm{s}}} = \frac{n}{n \bullet t}(S_{33}tp/A_{\mathrm{s}} + d_{33}V) = S_{33}p/A_{\mathrm{s}} + \frac{d_{33}}{t}V \tag{3}$$

where l_{s} is length of the stack, which equals the total thickness of all the piezoelectric wafers of the stack.

According to Hooke's law, the main stress σ_{s} and the strain has the relationship described as

$$\sigma_{\mathrm{s}} = E_{\mathrm{ps}}\varepsilon_{\mathrm{s}} \tag{4}$$

where E_{ps} is the elastic modulus of the piezoelectric material. Defining F_{a} as the internal axial force of the stack, we can obtain

$$\sigma_{\mathrm{s}} = \frac{F_{\mathrm{a}}}{A_{\mathrm{s}}} \tag{5}$$

Substituting Eq. (3) and Eq. (4) into Eq. (5), we can get

$$F_{\mathrm{a}} = E_{\mathrm{ps}}\varepsilon_{\mathrm{s}}A_{\mathrm{s}} = E_{\mathrm{ps}}\left(S_{33}p + \frac{d_{33}}{t}A_{\mathrm{s}}V\right) \tag{6}$$

Since the stack is constrained by the Π shape pedestal with the pre-compression screw, actuating moment will be generated. When PISA is incorporated with host structure, the actuating moment will act on the structure, which can be presented as

$$M_{\mathrm{a}}(t) = F_{\mathrm{a}} h = E_{\mathrm{ps}} h \left(S_{33} p + \frac{d_{33}}{t} V(t) \right) \tag{7}$$

where h is the height of PISA, which is defined as the distance from the axis of the stack to the bottom of PISA as shown in Fig. 1.

Equation (7) indicates the proportional relationship among the actuating moment and the height of the PISA, the pre-compression force, and the driving voltage.

3 Vibration Control Simulation of Cantilever Beam Using PISA

3.1 Piezoelectric active vibration control system modeling

The analogy relationship between inverse piezoelectric effect and thermal elastic effect was first presented by Freed in 1997[9]. Based on this analogy theory the inverse piezoelectric analysis can be simulated by thermal elastic analysis.

Assume an undamped vibration control system

$$\boldsymbol{M}\ddot{\boldsymbol{x}} + \boldsymbol{K}\boldsymbol{x} = \boldsymbol{f} \tag{8}$$

where $\boldsymbol{x} \in \mathbf{R}^n$ represents the displacement vector of the structure, $\boldsymbol{f}$ is the control force vector, and $\boldsymbol{M}$ and $\boldsymbol{K}$ represent the mass and stiffness matrices of the structure, in which the mass and stiffness contributions of piezoelectric material have already been considered. Based on the thermal-elastic analogy, an equivalent thermal expansion coefficient $\alpha = d_{33}/t$ needs to be defined. Using the theory of thermal-elastic analysis, a Ritz vector $\boldsymbol{S}_t$ can be obtained when a unit change of temperature load is applied to the structure. This vector can be equivalent to the Ritz vector induced by unit driving voltage applied to a piezoelectric actuator. In general, one Ritz vector is required for each piezoelectric actuator. Then the actuating force can be written as

$$\boldsymbol{f} = \boldsymbol{K}\boldsymbol{S}_t V \tag{9}$$

where V represents the driving voltage applied on the actuator.

Define the first coordinate transformation equation.

$$\boldsymbol{x} = [\boldsymbol{\Phi} \quad \boldsymbol{S}_t] \begin{Bmatrix} \boldsymbol{z} \\ \boldsymbol{z}_{\mathrm{r}} \end{Bmatrix} \tag{10}$$

where $\boldsymbol{\Phi}$ is the normalized eigenvector matrix of Eq. (8) with respect to generalized mass. Substituting Eq. (9) and Eq. (10) into Eq. (8) and multiply both sides of Eq. (8) by $[\boldsymbol{\Phi} \quad \boldsymbol{S}_t]^{\mathrm{T}}$ gives

$$\begin{bmatrix} \boldsymbol{I} & \boldsymbol{M}_{\mathrm{r}} \\ \boldsymbol{M}_{\mathrm{r}}^{\mathrm{T}} & \boldsymbol{M}_{\mathrm{rr}} \end{bmatrix} \begin{Bmatrix} \ddot{\boldsymbol{z}} \\ \ddot{\boldsymbol{z}}_{\mathrm{r}} \end{Bmatrix} + \begin{bmatrix} \boldsymbol{\Lambda} & \boldsymbol{K}_{\mathrm{r}} \\ \boldsymbol{K}_{\mathrm{r}}^{\mathrm{T}} & \boldsymbol{K}_{\mathrm{rr}} \end{bmatrix} \begin{Bmatrix} \boldsymbol{z} \\ \boldsymbol{z}_{\mathrm{r}} \end{Bmatrix} = \begin{Bmatrix} \boldsymbol{K}_{\mathrm{r}} \\ \boldsymbol{K}_{\mathrm{rr}} \end{Bmatrix} V \tag{11}$$

where $\boldsymbol{M}_{\mathrm{r}} = \boldsymbol{\Phi}^{\mathrm{T}}\boldsymbol{M}\boldsymbol{S}_t$, $\boldsymbol{M}_{\mathrm{rr}} = \boldsymbol{S}_t^{\mathrm{T}}\boldsymbol{M}\boldsymbol{S}_t$, $\boldsymbol{K}_{\mathrm{r}} = \boldsymbol{\Phi}^{\mathrm{T}}\boldsymbol{K}\boldsymbol{S}_t$, $\boldsymbol{K}_{\mathrm{rr}} = \boldsymbol{S}_t^{\mathrm{T}}\boldsymbol{K}\boldsymbol{S}_t$, and $\boldsymbol{I}$ is an identity matrix. Assume that only the first m order of normal modes are extracted. Then we obtain $\boldsymbol{\Phi} \in \mathbf{R}^{n\times m}$ and $\boldsymbol{\Lambda} \in \mathbf{R}^{m\times m}$.

The Ritz vector obtained from thermal-elastic analysis is a static result which makes Eq. (11) a stiff equation. In order to eliminate the ill condition of this stiff equation, the second coordinate transformation has to be made by the following equation:

$$\begin{Bmatrix} \boldsymbol{z} \\ \boldsymbol{z}_{\mathrm{r}} \end{Bmatrix} = \boldsymbol{W} \begin{Bmatrix} \boldsymbol{\eta} \\ \boldsymbol{\eta}_{\mathrm{r}} \end{Bmatrix} \tag{12}$$

where $\boldsymbol{W}$ is the right singularity matrix of $\bar{\boldsymbol{M}} = \begin{bmatrix} \boldsymbol{I} & \boldsymbol{M}_{\mathrm{r}} \\ \boldsymbol{M}_{\mathrm{r}}^{\mathrm{T}} & \boldsymbol{M}_{\mathrm{rr}} \end{bmatrix}$. Using Eq. (12), we have

$$\begin{bmatrix} \boldsymbol{\sigma} & \boldsymbol{0} \\ \boldsymbol{0} & \boldsymbol{0} \end{bmatrix} \begin{Bmatrix} \ddot{\boldsymbol{\eta}} \\ \ddot{\boldsymbol{\eta}}_{\mathrm{r}} \end{Bmatrix} + \begin{bmatrix} \boldsymbol{k} & \boldsymbol{k}_{\mathrm{r}} \\ \boldsymbol{k}_{\mathrm{r}}^{\mathrm{T}} & \boldsymbol{k}_{\mathrm{rr}} \end{bmatrix} \begin{Bmatrix} \boldsymbol{\eta} \\ \boldsymbol{\eta}_{\mathrm{r}} \end{Bmatrix} = \begin{Bmatrix} \boldsymbol{b} \\ \boldsymbol{b}_{\mathrm{r}} \end{Bmatrix} V \tag{13}$$

where $\boldsymbol{\sigma}$ is the non-zero singularity value matrix of $\bar{\boldsymbol{M}}$. Let $\boldsymbol{U}$ be the left singularity matrix of $\bar{\boldsymbol{M}}$, then

$$\begin{bmatrix} \boldsymbol{k} & \boldsymbol{k}_{\mathrm{r}} \\ \boldsymbol{k}_{\mathrm{r}}^{\mathrm{T}} & \boldsymbol{k}_{\mathrm{rr}} \end{bmatrix} = \boldsymbol{U}^{\mathrm{T}} \begin{bmatrix} \boldsymbol{\Lambda} & \boldsymbol{K}_{\mathrm{r}} \\ \boldsymbol{K}_{\mathrm{r}}^{\mathrm{T}} & \boldsymbol{K}_{\mathrm{rr}} \end{bmatrix} \boldsymbol{W} \tag{14}$$

$$\begin{Bmatrix} \boldsymbol{b} \\ \boldsymbol{b}_{\mathrm{r}} \end{Bmatrix} = \boldsymbol{U}^{\mathrm{T}} \begin{Bmatrix} \boldsymbol{K}_{\mathrm{r}} \\ \boldsymbol{K}_{\mathrm{rr}} \end{Bmatrix} \tag{15}$$

Solve $\boldsymbol{\eta}_{\mathrm{r}}$ from the second equation of Eq. (13),

$$\boldsymbol{\eta}_{\mathrm{r}} = -\boldsymbol{k}_{\mathrm{rr}}^{-1}\boldsymbol{k}_{\mathrm{r}}^{\mathrm{T}}\boldsymbol{\eta} + \boldsymbol{k}_{\mathrm{rr}}^{-1}\boldsymbol{b}_{\mathrm{r}} V \tag{16}$$

Substituting Eq. (16) into the first equation of Eq. (13) and finally, we have

$$\boldsymbol{\sigma}\ddot{\boldsymbol{\eta}} + (\boldsymbol{k} - \boldsymbol{k}_{\mathrm{r}}\boldsymbol{k}_{\mathrm{rr}}^{-1}\boldsymbol{k}_{\mathrm{r}}^{\mathrm{T}})\boldsymbol{\eta} = (\boldsymbol{b} - \boldsymbol{k}_{\mathrm{r}}\boldsymbol{k}_{\mathrm{rr}}^{-1}\boldsymbol{k}_{\mathrm{r}}^{\mathrm{T}})V \tag{17}$$

Equation (17) is the reduced order model for the piezoelectric active vibration control system. The state space model of the active control system can be constructed from Eq. (17) according to Eqs. (18) and (19).

$$\boldsymbol{A} = \begin{bmatrix} \boldsymbol{0} & \boldsymbol{I} \\ -\boldsymbol{\sigma}^{-1}(\boldsymbol{k} - \boldsymbol{k}_{\mathrm{r}}\boldsymbol{k}_{\mathrm{rr}}^{-1}\boldsymbol{k}_{\mathrm{r}}^{\mathrm{T}}) & -\boldsymbol{\sigma}^{-1}\bar{\boldsymbol{C}} \end{bmatrix} \tag{18}$$

$$\boldsymbol{B}=\begin{bmatrix}\mathbf{0}\\ \boldsymbol{\sigma}^{-1}(\boldsymbol{b}-\boldsymbol{k}_{\mathrm{r}}\boldsymbol{k}_{\mathrm{rr}}^{-1}\boldsymbol{k}_{\mathrm{r}}^{\mathrm{T}})\end{bmatrix},$$

$$\boldsymbol{C}=[\boldsymbol{\Phi}\quad \boldsymbol{S}_t]\boldsymbol{W} \tag{19}$$

where $\bar{\boldsymbol{C}}$ is a given damping matrix.

The control ability of PISA is tested in the active vibration control of a cantilever beam. The dimensions of the beam and piezoelectric stack used in PISA are listed in Table 1. The PISA is attached to the root surface of the beam as shown in Fig. 3. The height from the beam surface to the axis of the stack is set to 10 mm.

Table 1 Dimension of the beam and the stack

	Length (mm)	Width (mm)	Thickness (mm)
Beam (Al)	300	20	1.5
Stack (PZT5H)	30	10	10.0

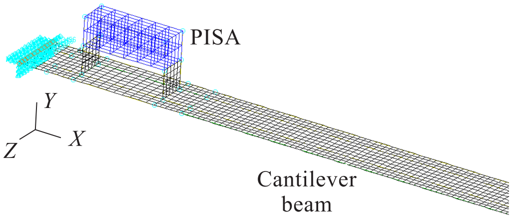

Fig. 3 Finite element model of cantilever beam bonded with PISA

3.2 Three control strategies

The positive position feedback control strategy was first proposed by Caughey and Goh in 1985[10]. A PPF controller has the same frequency spectral characteristic as a second order low pass filter, and its transfer function can be described as

$$G(s)=\frac{G_{\mathrm{a}}\omega^2}{s^2+2\zeta_{\mathrm{p}}\omega s+\omega^2} \tag{20}$$

where G_{a} and ζ_{p} is the gain and damping ratio of the controller.

In the PPF controller, the structural position information, for example, the tip point displacement response, is fed back to the PPF controller, and then the control signal will be generated by this controller. When it is applied in an active vibration control system, the parameters of the controller can be design according to the frequencies of zero and pole of the system[11,12].

The linear quadric regulator control is a classical control strategy which has been widely used in vibration control systems. In the design of LQR controller, the control force at the *i*-th time step depends upon the vibration response of the structure at that moment. To determine this control force for an optimal linear control, a cost function J is defined by

$$J=\frac{1}{2}\sum_{0}^{N}(\boldsymbol{x}_i^{\mathrm{T}}\boldsymbol{Q}\,\boldsymbol{x}_i+\boldsymbol{u}_i^{\mathrm{T}}\boldsymbol{R}\,\boldsymbol{u}_i) \tag{21}$$

where $\boldsymbol{Q}$ and $\boldsymbol{R}$ are weighting matrices. By minimizing the cost function J using Hamiltonian function, we can obtain the control signal,

$$\boldsymbol{u}_i=-(\boldsymbol{GPG}+\boldsymbol{R})^{-1}\boldsymbol{G}^{\mathrm{T}}\boldsymbol{F}_{\mathrm{s}}\boldsymbol{x}_i \tag{22}$$

$$\boldsymbol{G}=\boldsymbol{A}^{-1}(\boldsymbol{F}_{\mathrm{s}}-\boldsymbol{I})\boldsymbol{B} \tag{23}$$

$$\boldsymbol{F}_{\mathrm{s}}=\mathrm{e}^{A\Delta t} \tag{24}$$

where $\boldsymbol{P}$ is the steady state Riccati matrix given by

$$\boldsymbol{P}=\boldsymbol{Q}+\boldsymbol{F}_{\mathrm{s}}^{\mathrm{T}}\boldsymbol{P}(\boldsymbol{I}+\boldsymbol{GRG}^{\mathrm{T}}\boldsymbol{P})^{-1}\boldsymbol{F}_{\mathrm{s}} \tag{25}$$

The neural network predictive controller can output a control signal to make the response of a controlled system the same as a given reference signal. It uses a neural network model to predict future plant responses of the controlled system. In the controller an optimization algorithm gives the control signals to optimize future performance of the system. The neural network model is trained off-line in batch form using a chosen training algorithm[13,14].

The implementation of the NNP controller started from the training process of a neural network model for the piezoelectric active vibration control system. Then a constant value of zero is used as reference signal. The output of the system, which is also chosen to be the displacement response of the beam, will be controlled to follow this reference signal. Using this process the vibration response of the beam will be suppressed.

3.3 Simulation results

In the active vibration control simulation, the cantilever beam was excited by the sinusoidal signal with the frequency equal to the first bending mode frequency (15.63 Hz) of the beam. The PPF or NNP controller was set to be turned on automatically at $t=4$ s.

Figure 4 shows the tip point displacement response of the cantilever beam when the PPF control strategy was adopted. The result shows that the first bending mode response of the beam is suppressed by more than 60%.

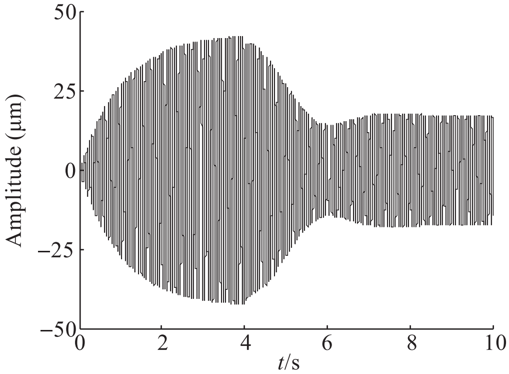

Fig. 4 Time history of tip point displacement response of the beam (the PPF controller was turned on at *t*=4 s)

Figures 5 and 6 show the tip point displacement responses of the beam when the LQR and NNP control strategies were adopted. The displacement amplitude of the first bending mode response was suppressed by 79% for the LQR strategy and more than 95% for the NNP strategy.

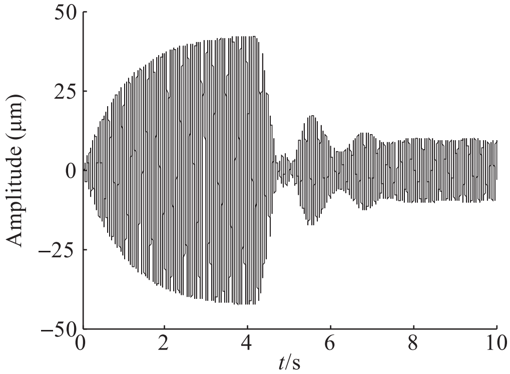

Fig. 5 Time history of tip point displacement response of the beam (the LQR controller was turned on at *t*=4 s)

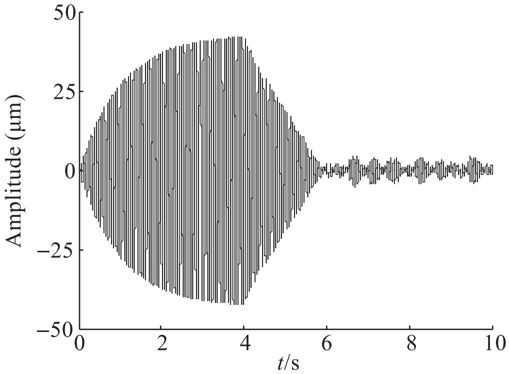

Fig. 6 Time history of tip point displacement response of the beam (the NNP controller was turned on at *t*=4 s)

Simulation results indicate that the bending mode response of cantilever beam can be saliently suppressed by using PISA.

4 Conclusions

With the purpose of exerting strong actuating power of piezoelectric stack and facilitating the incorporation of piezoelectric stack and host structure for vibration control application, a new type of piezoelectric stack actuator named PISA is developed. Simulation results indicate that PISA is an effective actuator for structural active vibration control. Besides, the manufacture cost will be reduced for its compact configuration design.

References

[1] Ramsay J V, Mugridge E G V. Barium titanate ceramics for fine-movement control. *Journal of Scientific Instruments*, 1962, **39**: 636-637.

[2] Bindal V, Chandra M. A piezoelectric displacement transducer for fine movement and its performance. *Indian Journal of Pure and Applied Physics*, 1977, **15**: 109-114.

[3] Dogan A, Xu Q, Onitsuka K, et al. High displacement ceramic metal composite actuators (Moonies). *Ferroelectrics*, 1994, **156**(1): 1-6.

[4] Dogan A, Fernandez J F, Uchino K, et al. The cymbal electromechanical actuator. *IEEE International Symposium on Applications of Ferroelectrics*, 1996, **1**: 213-216.

[5] Brennan M J, Garcia-Bonito J, Elliott S J, et al. Experimental investigation of different actuator technologies for active vibration control. *Smart Materials and Structures*, 1999, **8**: 145-153.

[6] Sugawara Y, Onitsuka K, Yoshikawa S, et al. Metal-ceramic composite actuators. *Journal of the American Ceramic Society*, 1992, **75**: 996-998.

[7] Zhu J, Wang D, Kirn C J, et al. Development of a mesoscale actuation device. In: Proceedings of the American Society of Mechanical Engineers Aerospace Division. New York, USA, 1996, **52**: 649-654.

[8] Zheng K, Yan S Z, Wen S Z, et al. Influence of preload on the piezoelectric for piezoelectric stack actuator. *Piezoelectric & Acoustooptics*, 2003, **25**(5): 363-365. (in Chinese)

[9] Freed B D, Babusk V. Finite element modeling of composite piezoelectric structures with MSC/NASTRAN. In: Proceedings of SPIE's 4th Annual SympFosiumon Smart Structures and Material: Smart Structure and Integrated Systems. San Diego, Califonia, 1997, **3041**: 676-688.

[10] Goh C, Caughey T K. On the stability problem caused by

infinite actuator dynamics in the collocated control of large space structure. *International Journal of Control*, 1985, **41**: 787-802.

[11] Gu H, Song G. Active vibration suppression of a composite I-beam using fuzzy positive position control. *Smart Materials and Structures*, 2005, **14**: 540-547.

[12] Yang Y M, Zhang H H, Hu Z. Positive position feedback based active vibration control of multiple modes. *Journal of Vibration Engineering*, 2005, **18**(3): 355-359. (in Chinese)

[13] The MathWorks, Inc. MATLAB User's Guide. Natick, MA, USA, Version 7.0.1.24704 (R14) Service Pack 1, 2004.

[14] Cai Z X. Intelligent Control: Fundamentals and Applications. 1st Ed. Beijing, China: National Defense Industry Press, 1998. (in Chinese)